

**EVOLUTION OF THE SOLAR AND CORONAL  
FIELD STRUCTURE: 1976 - 1991****S** DTIC  
ELECTE  
MAY 8 1992  
C DJ. Todd Hoeksema  
Center for Space Science and Astrophysics  
Stanford University  
Stanford, CA 94305  
U.S.A.**ABSTRACT**

The magnetic field of the Sun determines the structure of the corona and the interplanetary medium. Observations of the solar field made at the Wilcox Solar Observatory at Stanford from 1976 to the present have been used to model the field patterns in the corona, the source of the heliospheric magnetic field. The IMF polarity at Earth can be predicted with about 80% reliability throughout the solar cycle. However, the field in the ecliptic is just one slice of a three-dimensional structure that changes greatly during the solar cycle. Near solar minimum the heliospheric current sheet is confined to the Sun's equatorial region. As the polar fields decay and reverse near solar maximum, the geometry of the heliospheric field becomes much more complex. Model coronal fields can also be used to estimate the solar wind velocity, determine the solar origin of interplanetary structures, and predict the out-of-ecliptic component of the IMF at Earth.

**INTRODUCTION**

The interplanetary magnetic field has direct effects on the terrestrial system. The large-scale structure of the interplanetary medium largely depends on the arrangement of field in the photosphere. From the photospheric field the configuration of the field in the corona, at the base of the solar wind, can be computed. Using a uniform series of precise low-resolution solar magnetic field measurements began at the Wilcox Solar Observatory at Stanford in 1976, a model of the coronal and heliospheric field that spans one and a half solar activity cycles has been computed. In this paper the evolution of the field is described and comparisons are made between the field patterns in Solar Cycles 21 and 22.

DISTRIBUTION STATEMENT A

Approved for public release;  
Distribution Unlimited

02 4 06 084

92-08853



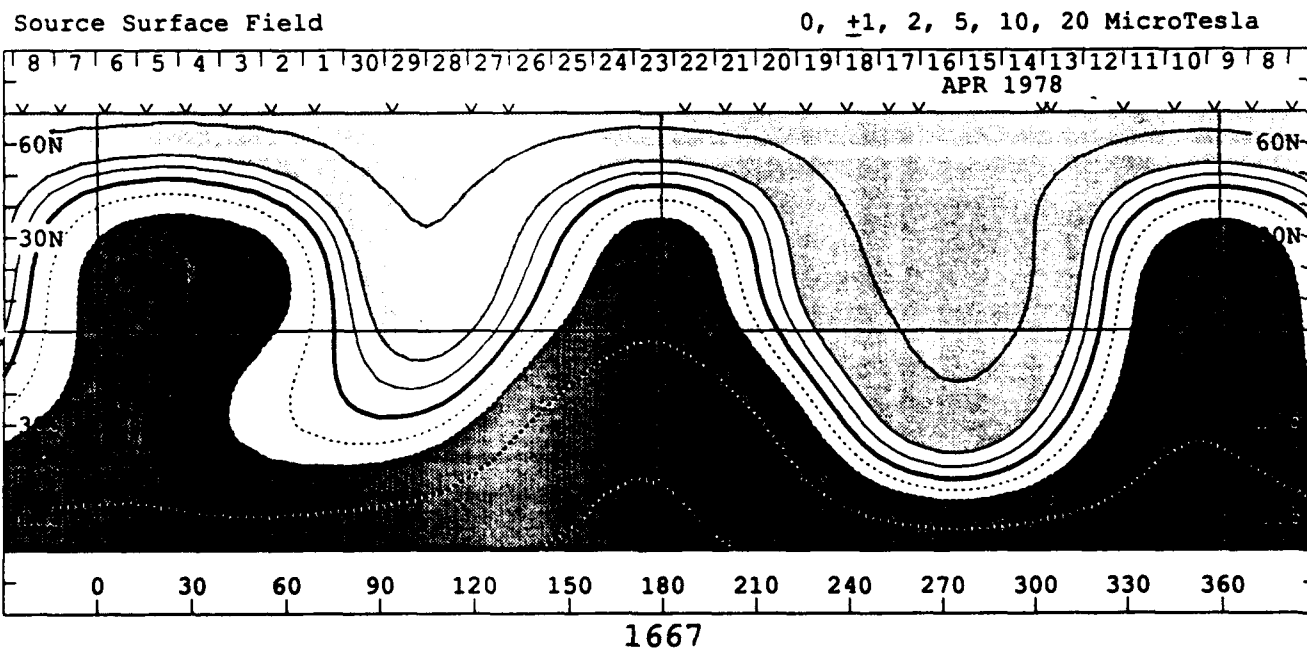
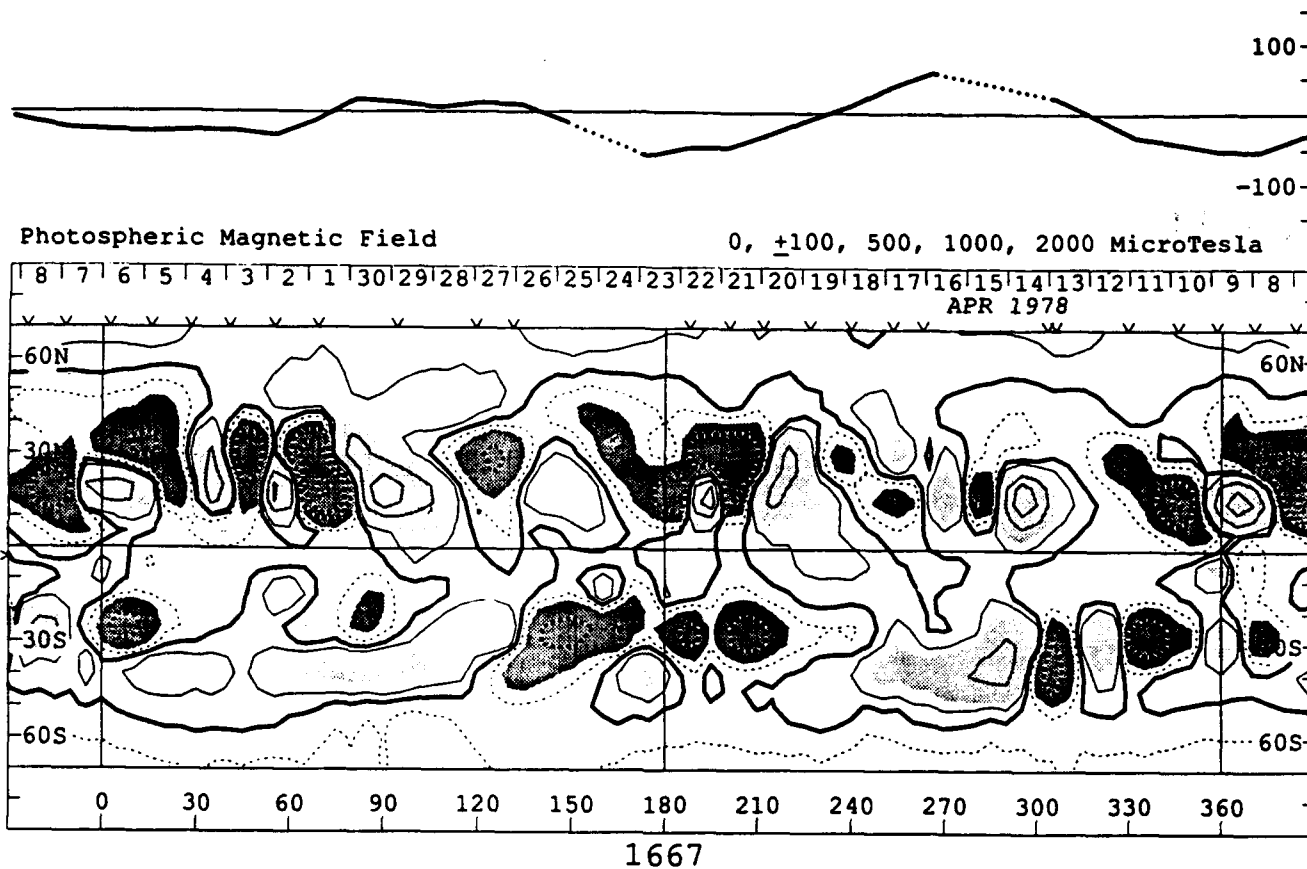


Figure 1: The upper panel shows the photospheric field for CR 1667 in April 1978. Fields greater than 2 Gauss (200 uT) are shaded lightly. Fields below -2 G are shaded more darkly. Central meridian dates are indicated on the upper axis, as are times of magnetograms. Time goes from right to left. Earth's latitude is indicated in the left margin. Field values are not well determined above 70°. The independently measured mean magnetic field of the Sun is shown at the top of the panel. B) The lower panel show the computed radial field at the 2.5 Rs source surface, in the same format. Contours and shading values are a factor of 100 smaller and the polarity structure is simpler. This pattern shows the configuration of the heliospheric IMF and generally agrees with observations.

The field is computed using a potential field – source surface model in which the field between two concentric spheres is calculated (e.g. Hoeksema, 1984 and references therein). The observations at the photosphere provide the lower boundary condition. To simulate the distortion of the field by the acceleration of the solar wind, the field is forced to be radial at 2.5 solar radii, the source surface, as the upper boundary condition. Under the assumption that the region between the two surfaces is current free, the potential is a scalar that can be described by Legendre polynomials. The vector field can be computed from derivatives of the potential. At the source surface the field is purely radial, by assumption. Figure 1 shows the photospheric field (top) and computed source surface field (bottom) for Carrington Rotation 1667.

To a first approximation, the polarity pattern at the source surface is carried radially outward by the solar wind and changes only slightly above that height, in the absence of dynamical effects. Dynamical effects increasingly distort the shape of the heliospheric current sheet with increasing distance from the Sun (Behannon et al., 1989). Comparison between the polarity structure computed at the source surface and observed in the ecliptic shows that the model predicts the correct daily polarity about 80% of the time (Hoeksema, 1983, 1984).

### THE HELIOSPHERIC FIELD

The heliospheric field changes greatly during the solar cycle. Figure 2 shows the evolution of the field over a 15 year time interval from 1976 to the present. Here a two rotation wide window is shown in each panel. The panels are centered seven rotations apart. While some time periods are not shown, it is still possible to see the continuity of the largest features over very long time periods. At solar minimum, in 1976, the current sheet was basically equatorial. The polar fields at that time were very strong and there was little activity. As the cycle progressed the current sheet became more warped, rising to higher and higher latitudes. During the rise to maximum the complexity of the structures increased, the current sheet often reached the poles, and occasionally small isolated regions of reversed polarity were present (e.g. CR 1677 and CR 1698). In 1980 the polar fields reversed and the patterns began to simplify. During the declining phase of the cycle, the heliospheric field became more and more dipolar in nature (tilted in 1982 and 1984) and was basically flat again in 1986. During the rise of Cycle 22, which began in 1987, similar variations are seen. The polar fields weakened and had again reversed by late 1990.

Statement A per telecon  
 Dr. Neal Sheeley ONR/Code 1114  
 Arlington, VA 22217-5000

NWW 5/7/92



NTIS Grant	<input checked="" type="checkbox"/>
DTIC TAB	<input type="checkbox"/>
Unannounced	<input type="checkbox"/>
Justification	
By _____	
Distribution/	
Availability Codes	
Dist	Avail and/or Special
A-1	

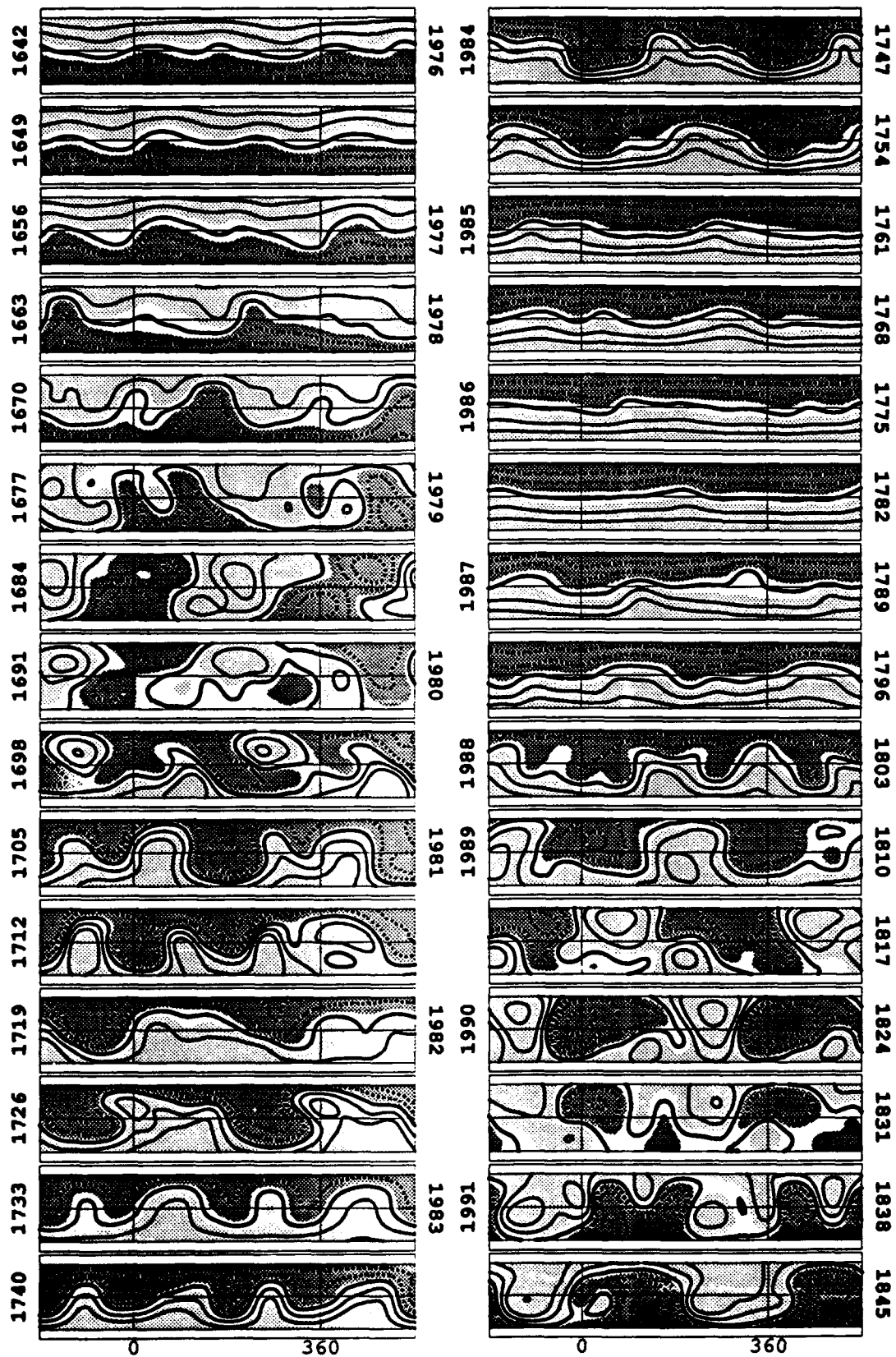


**Figure 2:** Each panel shows a two Carrington Rotation wide map of the computed coronal magnetic field centered on the rotation indicated in the outer margin. The shading levels are the same as in Fig. 1b. Every seventh rotation is shown. The first rotation shown in a year is labeled in the inner region.

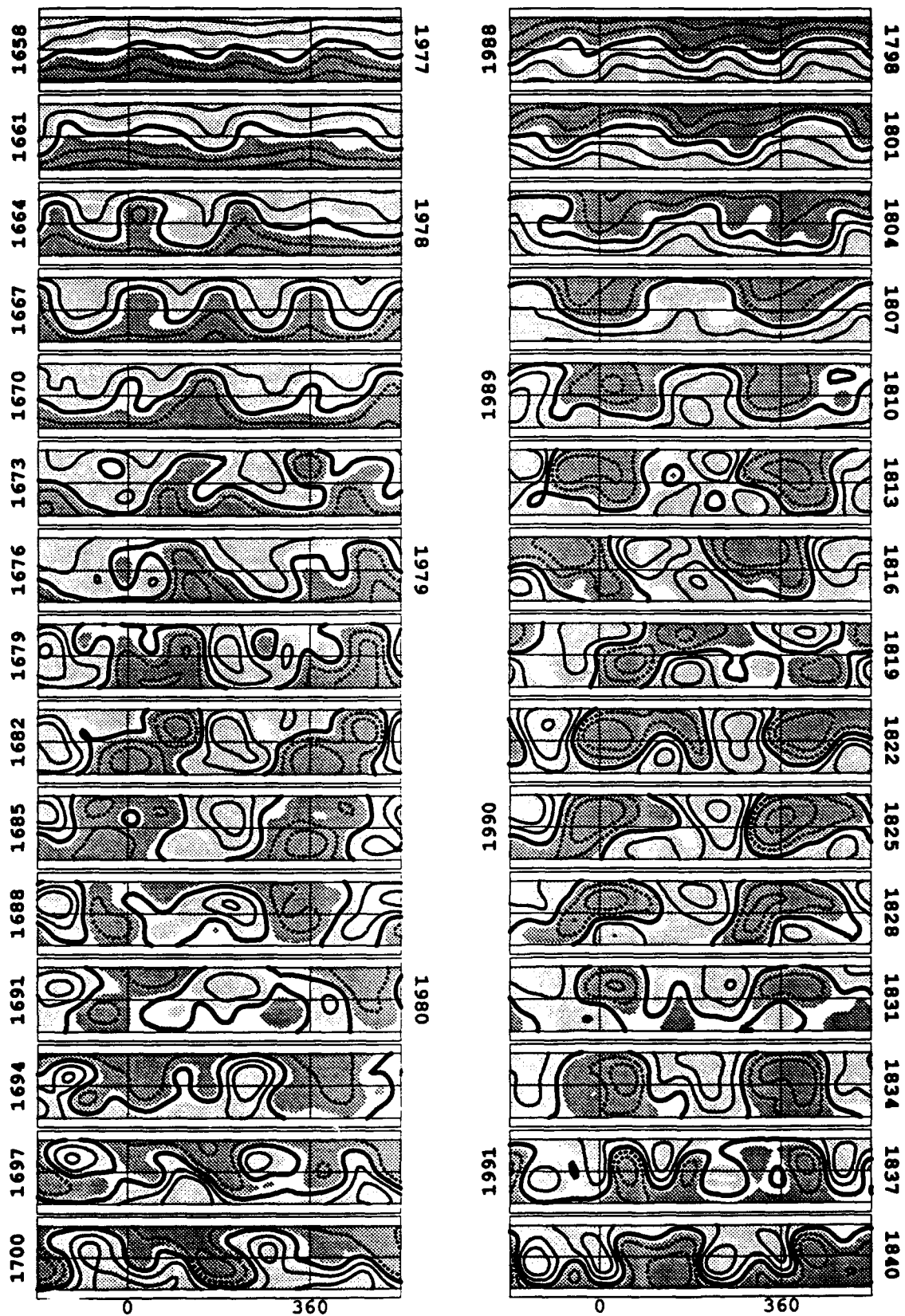


Figure 3: The panels are similar to those in Figure 2, but are centered on every third rotation. The left column shows the rising and maximum phases of Solar Cycle 21; the right column is for Cycle 22. Carrington rotation boundaries are shown at the bottom. The similarities at comparable times during the cycles are striking. The most notable differences occur in 1978 and 1988-1989. Notice the long lifetimes of some features and the rotation rate, shown by the slope. The polar fields reverse near the bottom of each column.

A more detailed comparison of the two cycles can be seen in Figure 3. Here successive panels are centered only three rotations apart and it is easier to follow the evolution of individual features. One particularly long-lived example is the negative polarity feature that emerges in CR 1804 near 0 degrees and lives, with a few distortions and some gradual movement, through the end of the interval shown. Small isolated regions of opposite polarity can be identified in each cycle.

The overall similarity between the structures at comparable points in the two cycles is striking, e.g. CR 1661 & 1801, 1679 & 1819, 1688 & 1828, and 1700 & 1840. The differences between the two cycles are also very interesting. Compare the prominent 4-sector structure in CR 1664 - 1670 that did not have a counterpart in Cycle 22.

### CYCLE PARAMETERS

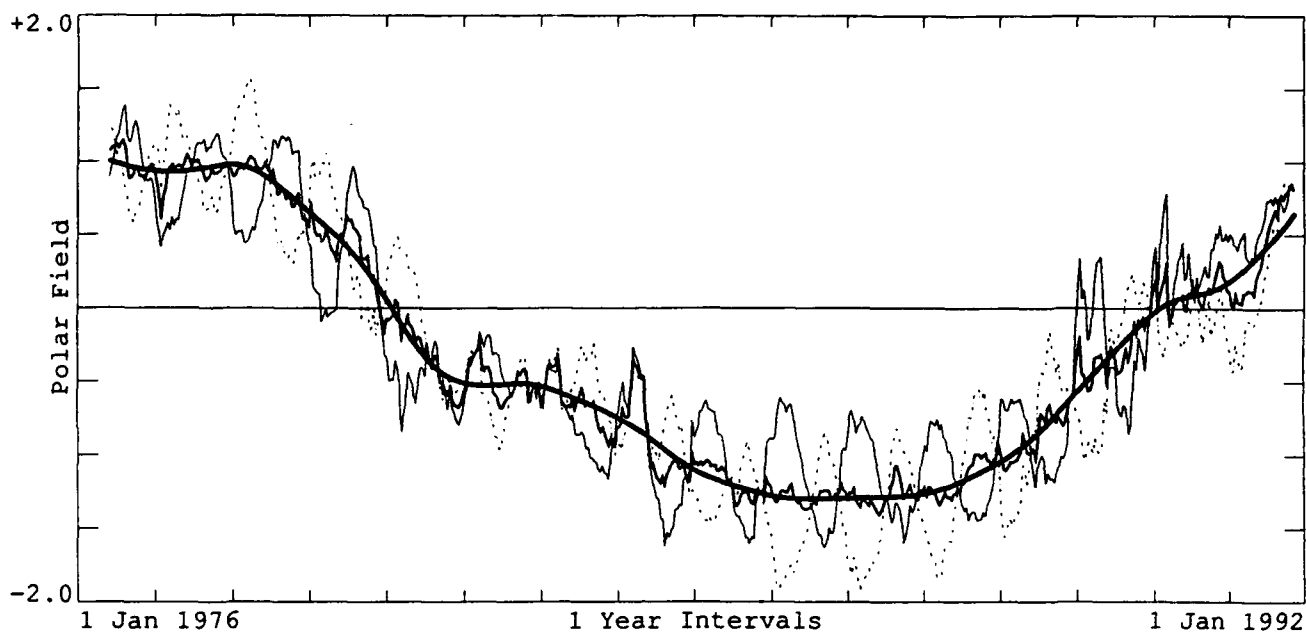
A variety of meaningful indices of the solar cycle can be defined from these data. The ones that may be important for the heliospheric field are the polar field strength and the maximum inclination of the current sheet. Figure 4 shows the evolution of two such parameters during the last 15 years.

The top panel shows the variation of the northern and southern polar fields and the smoothed average of the two. The polar field reversal in 1980 was stronger than the 1990 reversal. The field strength was about 25% greater at minimum in 1986 than in 1976. The bottom panel shows how the inclination of the heliospheric current sheet reaches a maximum for two or three years at solar maximum and gradually decreases toward minimum. The smaller inclination at minimum in 1986 is related to the increased polar field strength relative to the previous minimum.

### PREDICTIONS

Because the large scale field varies slowly and because the solar wind takes several days to travel from the Sun to the Earth, the model coronal field can be used to predict terrestrial conditions several days in advance. Figure 5 shows the source surface computed in the standard way in the upper panel. The lower panel shows a preliminary computation based on the same observations that extends nearly a full rotation farther. The subterrestrial field values for each date are indicated in the upper margin and could be used as predictions of the IMF field direction.

## Polar Field Strength vs. Time



## Maximum Inclination of Current Sheet

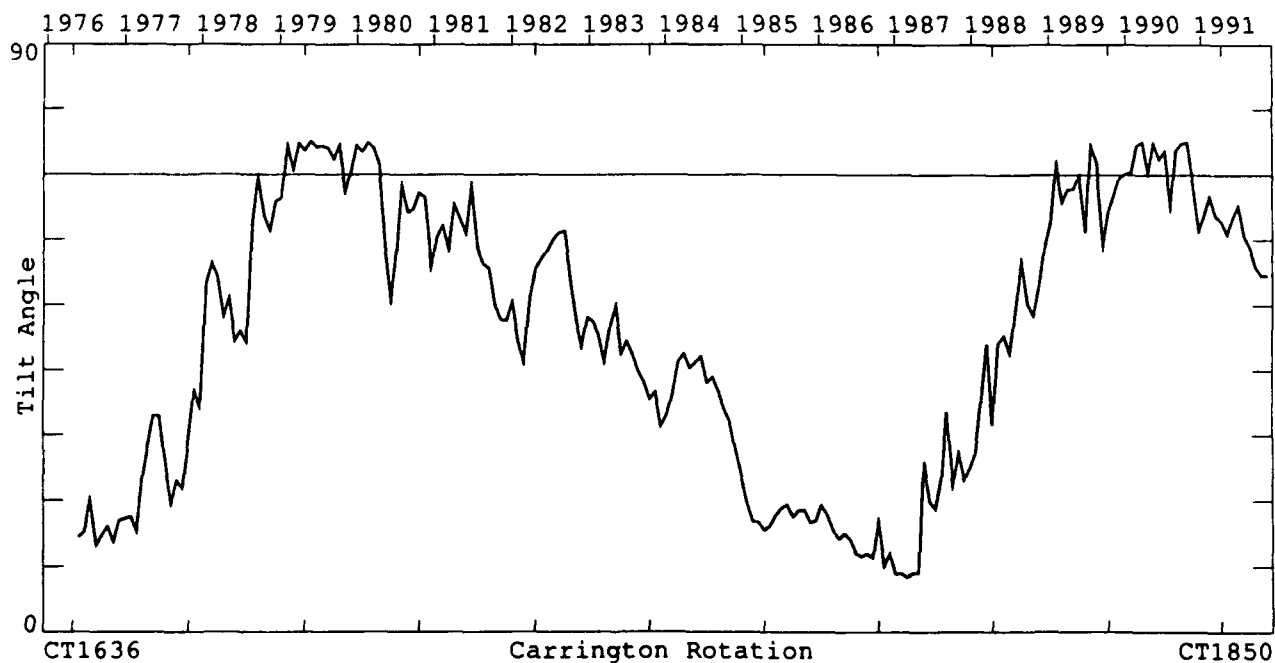
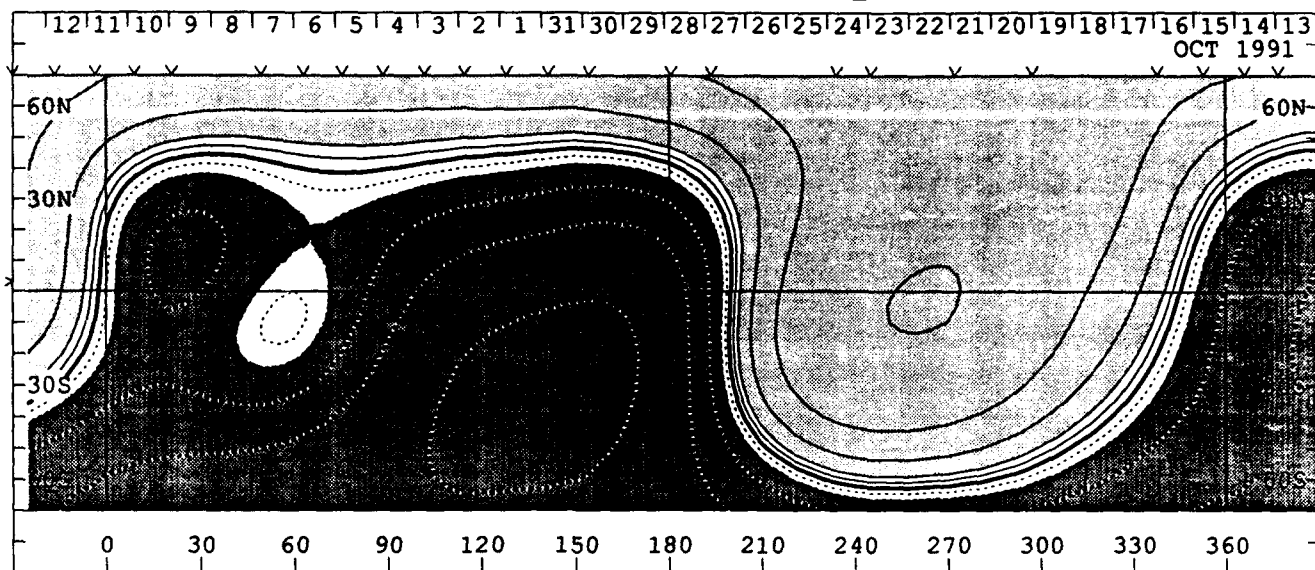


**Figure 4:** The top panel shows the variation of the polar field strength from 1976 to the present. The dark line is a smoothed average of the two poles. The lighter solid line shows the variation of the northern pole; the dashed line shows the negative of the southern polar field observations. The large annual variation is due to the inclination of the Earth's orbit to the solar equator. The average inclination of the heliospheric current sheet computed at 2.5 Rs is shown in the bottom panel. The variations of these quantities are related to changes in the photospheric field.

WILCOX SOLAR OBSERVATORY

Source Surface Field

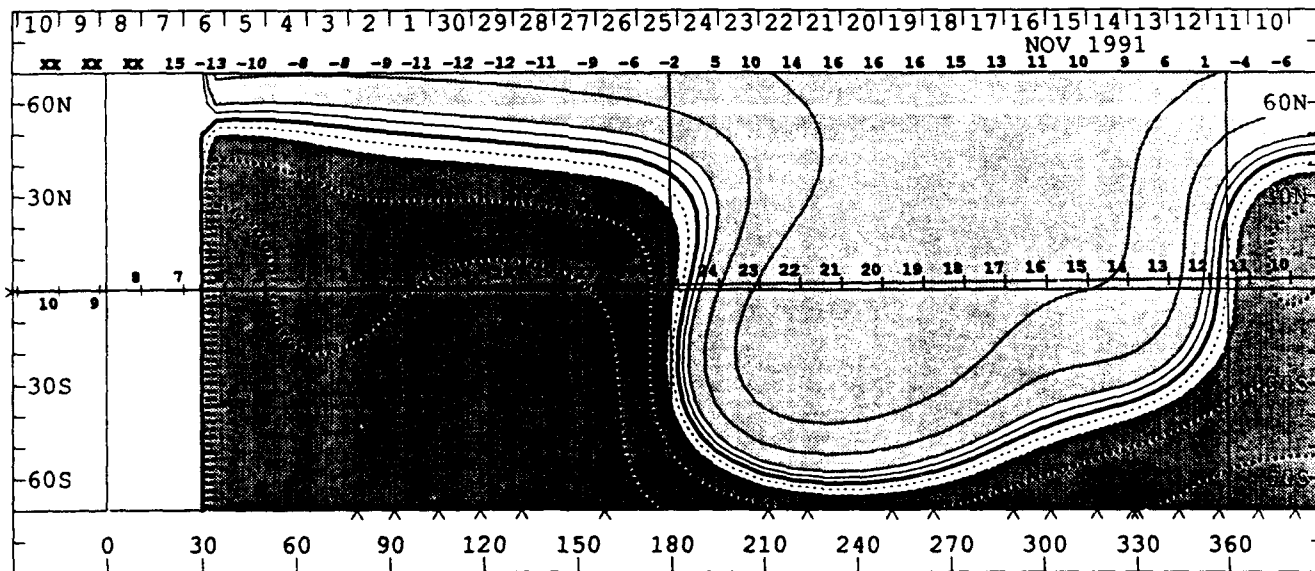
0, +1, 2, 5, 10, 20 MicroTesla



1848

Bsource.prelim field

0, +1, 2, 5, 10, 20 MicroTesla



1849

Figure 5: The upper panel shows the field at the source surface computed for Carrington Rotation 1848, similar to Figure 1. Notice that the last valid data were computed for CR 1849:325 (see blank space at left of panel.) The lower panel shows a preliminary computation of the field for the following rotation based on the same data, taken through 3 December, 1991. The labeled line in the center shows the path of the Earth; each date is labeled. The numbers listed near the top of the chart (near 75°) show the computed field strength at the source surface for the corresponding day. Field magnitudes above 2 are a good predictor of the IMF polarity. The computation is valid through a central meridian passage date of 5 December. Solar wind leaving the Sun at that time would not be expected to reach the Earth for 3 to 5 days.

These data can also be used to predict the solar wind velocity. Wang *et al.* (1990) have developed a model for predicting the solar wind speed based on the expansion factor of flux tubes between the photosphere and the source surface. According to that work, the less the a tube diverges, the greater the solar wind speed that originates from it. The agreement with ecliptic measurements is quite impressive. Out-of-ecliptic confirmation will await the results of the Ulysses spacecraft.

Hoeksema and Zhao (1992) and Zhao and Hoeksema (1992) have developed a method for predicting the orientation of the out-of-ecliptic IMF component for active region associated coronal mass ejections. Based on a limited analysis (only 11 cases so far) for which the solar source of a Bz event can be identified, they find that the field direction above the flare associated with a CME predicts the out-of-ecliptic component of the subsequent Bz event at Earth extremely well. This promises to be a fruitful area for further work.

## CONCLUSIONS

The large-scale structure of the heliospheric field can be computed from photospheric observations of the magnetic field. The field evolves from a roughly dipole like configuration at solar minimum to a complex state at solar maximum, when the polar fields reverse. In all parts of the solar cycle, there is a great deal of continuity in structure from one rotation to the next. These computations have been verified in the ecliptic plane and can be extended to other latitudes.

Plots of the photospheric data, source surface model fields, and harmonic coefficients are now available for use in other studies (Hoeksema and Scherrer, 1986 and Hoeksema, 1991).

These computations are useful not only for description, but also for prediction. Combining quick reduction of data with model calculations promises eventually to provide advance predictions of solar wind polarity and speed. Advance warning of the out-of-ecliptic component of the field associated with flare-associated CMEs may also be possible.

*Acknowledgement:* This work was supported in part by NASA Grant NGR-559, ONR Contract N00014-89-J-1024 and NSF Grant ATM 90-22249.

## REFERENCES

- Behannon, K.W., L.F. Burlaga, J.T. Hoeksema, and L.W. Klein, Spatial Variation and Evolution of Heliosphere Sector Structure, *J. Geophys. Res.*, **94**, 1245, 1989.
- Hoeksema, J.T., Structure and Evolution of the Large Scale Solar and Heliospheric Magnetic Fields, *CSSA-ASTRO-84-07, Ph.D. Diss.*, Stanford University, 1984.
- Hoeksema, J.T. and P.H. Scherrer, The Solar Magnetic Field - 1976 through 1985, WDC-A for Sol-Terr. Phys., *Rpt. UAG-94*, 1986.
- Hoeksema, J.T., The Solar Magnetic Field 1985 Through 1990, *CSSA Rpt. CSSA-ASTRO-91-01*, 1991.
- Hoeksema, J.T., J.M. Wilcox, P.H. Scherrer, Structure of the Heliospheric Current Sheet in the Early Portion of Sunspot Cycle 21 *J. Geophys. Res.*, **87**, 10331, 1982.
- Hoeksema, J.T., J.M. Wilcox, P.H. Scherrer, The Structure of the Heliospheric Current Sheet: 1978-1982, *J. Geophys. Res.*, **88**, 9910, 1983.
- Hoeksema, J.T. and X. Zhao, Prediction of Magnetic Orientation in Driver Gas-Associated -Bz Events, *J. Geophys. Res.*, in press, 1992.
- Wang, Y.-M., N.R. Sheeley, Jr., and A.G. Nash, Latitudinal distribution of solar-wind speed from magnetic observations of the Sun, *Nature*, **347**, 439, 1990.
- Zhao, X. and J.T. Hoeksema, Identification of Driver Gas - Associated Bz Events and Prediction of Their Orientation, this proceedings, 1992.